Interlocked Systems

International Edition: DOI: 10.1002/anie.201509702
German Edition: DOI: 10.1002/ange.201509702

Synthesis and Dynamics of Nanosized Phenylene–Ethynylene–Butadiynylene Rotaxanes and the Role of Shape Persistence

Christopher Schweez[+], Philip Shushkov[+], Stefan Grimme, and Sigurd Höger**

Abstract: *Phenylacetylene-based [2]rotaxanes were synthesized by a covalent-template approach by aminolysis of the corresponding prerotaxanes. The wheel and the bulky stoppers are made of phenylene–ethynylene–butadiynylene macrocycles of the same size. The stoppers are large enough to enable the synthesis and purification of the rotaxane. However, the wheel unthreads from the axle at elevated temperatures. The deslipping kinetics and the activation parameters were determined. We described theoretically the unthreading by state-of-the-art DFT-based molecular-mechanics models and a string method for the simulation of rare events. This approach enabled us to characterize in detail the unthreading mechanism, which involves the folding of the stopper during its passage through the wheel opening, a process that defies intuitive geometrical considerations. The conformational and energetic features of the transition allowed us to infer the molecular residues controlling the disassembly timescale.*

Molecular nanotechnology, which aims to build artificial molecular assemblies that mimic the function of sophisticated biological complexes,[1] has relied upon the development of mechanically interlocked molecules, such as rotaxanes, catenanes, and pretzel-shaped molecules, for nearly half a century.[2] Such mechanically interlocked molecules have been used to design various miniature devices, including switches, shuttles, elevators, and even protein-synthesizing machines similar to the ribosome.[3] Understanding of the persistence of shape has been mandatory for the design of nanoarchitectures and the function of molecular machines.

Many synthetic methods for the preparation of rotaxanes have been reported. Often templates have been used to increase the efficiency of the synthesis by organizing the reactants.[4] These templates generally utilize various weak interactions and supramolecular concepts.[5–8] The covalent-template approach, which was often employed in the early days of rotaxane synthesis,[9] has received considerable attention recently because of the emergence of novel synthetic methods for the development of extended structures.[10–13] In particular, also terephthalic acid derivatives have been described as templates for the construction of rotaxanes based on shape-persistent phenylacetylene macrocycles, but this attempt was not successful.[14]

Besides the intricate synthetic pathways, rotaxanes exhibit distinctive molecular dynamics, which can be characterized by several timescales.[15] These dynamics include the relative motion of the rotaxane constituents and the spontaneous disassembly of the complex, which gives rise to novel methods for building molecular assemblies but at the same time hampers the rotaxane function by disengaging the molecular parts.

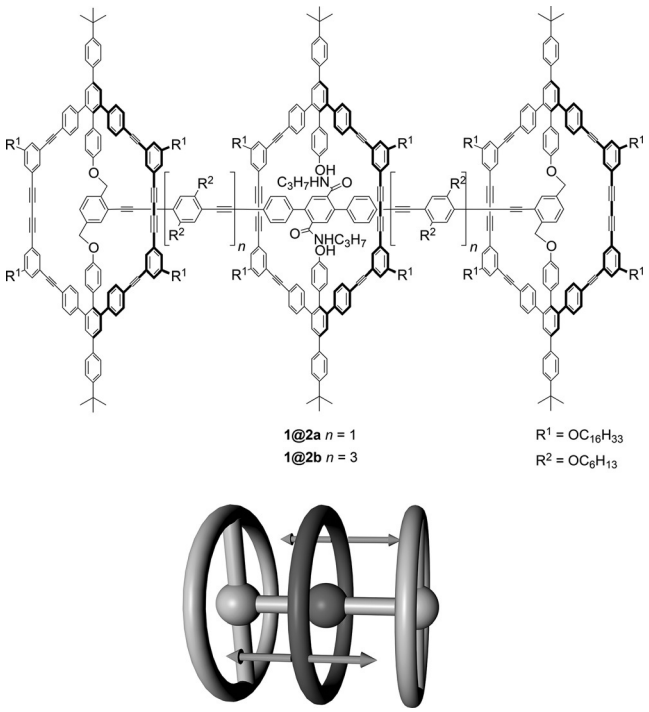

Figure 1. Top: Two novel [2]rotaxanes, **1@2a** and **1@2b**, based on shape-persistent macrocycles. Bottom: Illustration of the short-term dynamic behavior of the [2]rotaxane: the shuttling of the wheel along the axis.

[*] C. Schweez,[+] Prof. Dr. S. Höger
Kekulé Institut für Organische Chemie und Biochemie
Rheinische Friedrich-Wilhelms-Universität Bonn
Gerhard-Domagk-Strasse 1, 53121 Bonn (Germany)
E-mail: hoeger@uni-bonn.de
Dr. P. Shushkov,[+] Prof. Dr. S. Grimme
Mulliken Center for Theoretical Chemistry
Institut für Physikalische und Theoretische Chemie
Rheinische Friedrich-Wilhelms-Universität Bonn
Beringstrasse 4, 53115 Bonn (Germany)
E-mail: grimme@thch.uni-bonn.de
[+] These authors contributed equally.

Supporting information for this article is available on the WWW under http://dx.doi.org/10.1002/anie.201509702.

Shape-persistent phenylacetylene macrocycles have attracted considerable interest during the last two decades because their rigidity allows the formation of structures with predictable shape and defined positioning of functional groups.[16] The building blocks of the ring are rather rigid, and they are connected in such a way that the target structure is thought to be unfoldable under normal conditions.

We report herein a covalent-template approach for the modular and tailored synthesis of the nanosized phenylene–ethynylene–butadiynylene rotaxanes **1@2a** and **1@2b** (Figure 1) with different axis lengths. This approach builds upon our earlier work on template-directed synthesis[17,18] and should in principle enable the preparation of even more complex mechanically interlocked molecules, of which we show herein the first examples. The rotaxane features the wheel **1** and the stopper–axis building blocks **2a** and **2b**. Both the rotaxane wheel and the stoppers are shape-persistent macrocycles of the same size, which together with the occupied wheel interior and the *tert*-butylphenyl and alkoxy groups at the ring exterior are expected to guarantee that the wheel could not leave the axis. However, the rotaxane, surprisingly, disassembles spontaneously. Accordingly, we report a detailed theoretical investigation of the unthreading of the wheel from the rotaxane axis. This analysis helped us deduce the molecular residues that control the stability and the mechanics of this molecular assembly.

The synthetic route towards the [2]rotaxanes is shown in Scheme 1. The macrocycles **3** and **7** are obtained by template-directed syntheses of the half-rings[17] and the template molecules (see the Supporting Information). To avoid the steric repulsion between the central wheel macrocycle and the terminal stopper macrocycles, the monoprotected bisacetylene spacers **4a** and **4b** were attached to **3** by a twofold coupling reaction under standard conditions to give **5a** in quantitative yield and **5b** in good yield. Subsequent deprotection with tetra-*n*-butylammonium fluoride (TBAF) in the presence of water (4 vol%) avoided the undesired cleavage of the ester bonds.[18] The resulting compound **6** was then

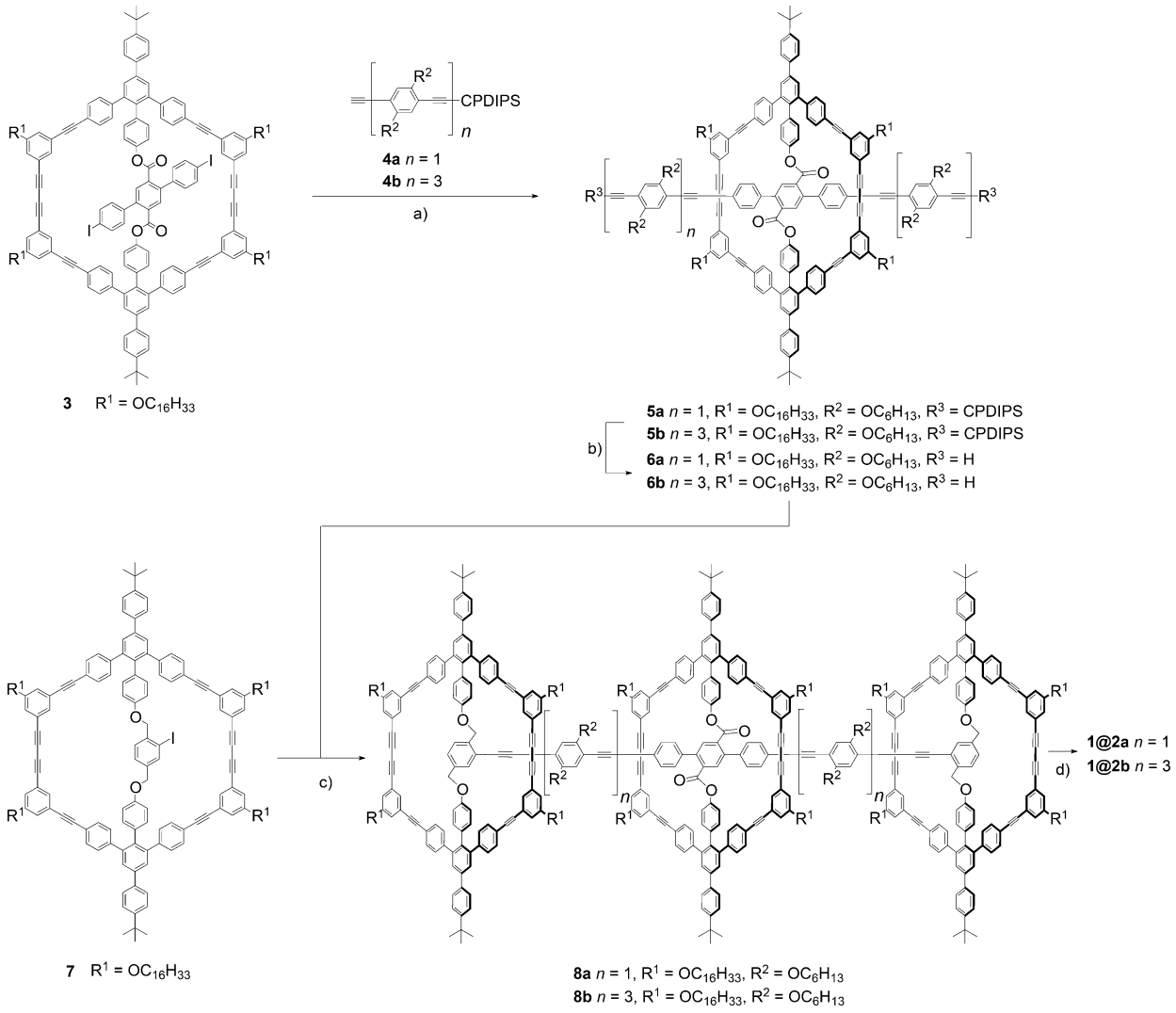

Scheme 1. a) $[PdCl_2(PPh_3)_2]$, CuI, PPh_3, THF, NEt_3, 60 °C, 18 h, **5a**: quant., **5b**: 51%; b) TBAF, H_2O (4 vol%), THF, room temperature, 50 h, **6a**: 61%, **6b**: 96%; c) $[PdCl_2(PPh_3)_2]$, CuI, toluene, NEt_3, 100 °C, 18 h, **8a**: 38%, **8b**: 22%; d) *n*-propylamine, NH_4Cl, THF, 50 °C, 16 h, **1@2a**: 21%, **1@2b**: 13%. CPDIPS = (3-cyanopropyl)diisopropylsilyl.

coupled with the macrocycle **7** in a double Sonogashira–Hagihara reaction with $[PdCl_2(PPh_3)_2]$ and CuI in toluene and NEt_3 at 100 °C to yield the [2]prerotaxane **8a** in 38 % yield or **8b** in 22 % yield, both of which were purified by column chromatography and preparative recycling GPC (recGPC).

In the [2]prerotaxanes, the macrocyclic stoppers **7** are covalently attached through benzylic ether bonds to the axis, whereas the wheel macrocycle is connected through phenolic ester bonds to the axis, which allows selective bond cleavage at the carboxy group by nucleophilic substitution. The [2]rotaxane **1@2** was therefore prepared by aminolysis with *n*-propylamine. Purification by preparative recycling GPC gave the [2]rotaxanes **1@2** as yellow solids in surprisingly low yields (**1@2a**: 21 %; **1@2b**: 13 %). Both rotaxanes dissolve well in dichloromethane, chloroform, and THF, and the successful syntheses were confirmed by ^{1}H NMR spectroscopy, MALDI-TOF MS, and GPC analysis (see the Supporting Information).

The observed low yields can be explained by the presence of the free rotaxane wheel **1** and axes **2a** and **2b**, which were isolated from the reaction mixture in addition to the [2]rotaxanes, as determined by GPC and MS. The presence of the disassembled rotaxane components might be attributed to the formation of two precursor isomers as already proposed by Morin and co-workers (Figure 2).[14] Only isomer **A** leads to rotaxane formation, whereas isomer **B** generates after aminolysis the free wheel and the stopper–axis unit. However, neither NMR spectroscopy nor chromatographic methods indicated the presence of two isomers. Attempts to separate the isomers of **8** by recGPC were unsuccessful, and their existence remains uncertain. Thus, the separation into the components could be the result of an unthreading during the aminolysis reaction.

Further experimental observations of the pure rotaxane showed the appearance of additional signals in the GPC and mass spectrum after solutions of **1@2a** and **1@2b** were kept for a prolonged time at room temperature. MS analysis of these samples confirmed the presence of the free wheel **1** and axes **2a** and **2b** besides the [2]rotaxanes, and the absence of any other decomposition products (see the Supporting Information). This observation suggests that the wheel unthreads from the axis by a slow deslipping process.[19,20] However, despite the plausibility of the unthreading process, it poses a mechanical puzzle: the stoppers are shape-persistent macrocycles that are identical to the wheel by design, which should make it highly improbable for the wheel to slip off the axis.

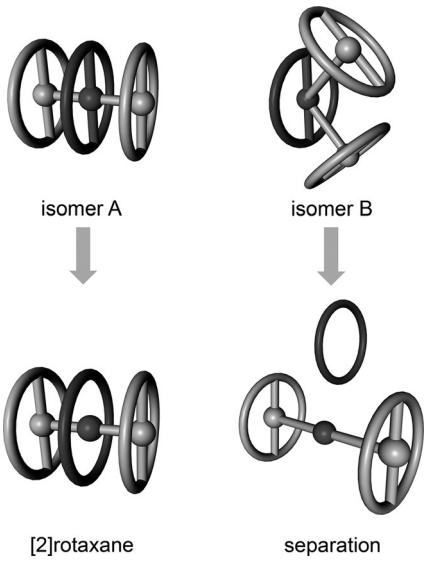

Figure 2. Precursor isomers. Only isomer A features prerotaxane geometry. The aminolysis of isomer A leads to the desired [2]rotaxane, whereas isomer B generates the free wheel and axis.

The deslipping process of the [2]rotaxane **1@2a** was analyzed at elevated temperatures in THF by recGPC, which allowed the separation of the [2]rotaxane, the axis, and the free wheel. From the rate constants at different temperatures (half-lives $\tau_{1/2}$: 33 h/323 K; 8.7 h/333 K; 6.6 h/338 K), the activation barrier is estimated to be around (24 ± 4) kcal mol^{-1} (see the Supporting Information).

To gain further insight into the mechanism of unthreading, we described theoretically the rotaxane deslipping reaction. A simplified rotaxane complex was investigated with the long alkyl side chains of the macrocycles, which influence primarily the solubility of the complex, replaced by methyl groups. All atoms of the rotaxane were accounted for explicitly, whereas the solvent, tetrahydrofuran, was treated implicitly by a customized generalized Born model including an energetic contribution proportional to the molecular surface.[21] Ab initio calculation of the rotaxane potential-energy surface in molecular dynamics (MD) is prohibitive owing to the large number of atoms (720 in total) in the system. Therefore, a customized molecular-mechanics force field (QMDFF) was parameterized on the basis of ab initio density functional theory calculations[22] (see the Supporting Information for details). Since direct simulation of the deslipping event is unfeasible, because the unthreading occurs over a very long timescale, as suggested by the high activation barrier, we applied the finite-temperature string method,[23] which represents the sequence of conformational events by a succession of equidistant images. The optimized string takes into account enthalpic effects, which give preference to the low-energy regions of the potential-energy surface, and entropic effects, which bias the path to flatter regions of the surface. A representative optimized path is shown in Figure 3, and further details of the computational method are deferred to the Supporting Information. For movies of the unthreading simulations, see Ref. [24].

The Gibbs free energy profile of the unthreading exhibits a few metastable minima separated by barriers corresponding to the major conformational bottlenecks (Figure 3 A). In the initial and final states of the process, the system assumes an extended conformation, in which both angles (depicted by the green vectors in Figure 3 B) between the stopper *tert*-butylphenyl groups are nearly straight. As the system moves along the transition path, a remarkable conformational rearrangement takes place: one of these angles gradually decreases, which correlates with the folding of the stopper, and as a result, the bulky moieties that otherwise stick out from the periphery of the stopper ring can fit within the opening of the wheel. This rearrangement is facilitated by the flexibility of

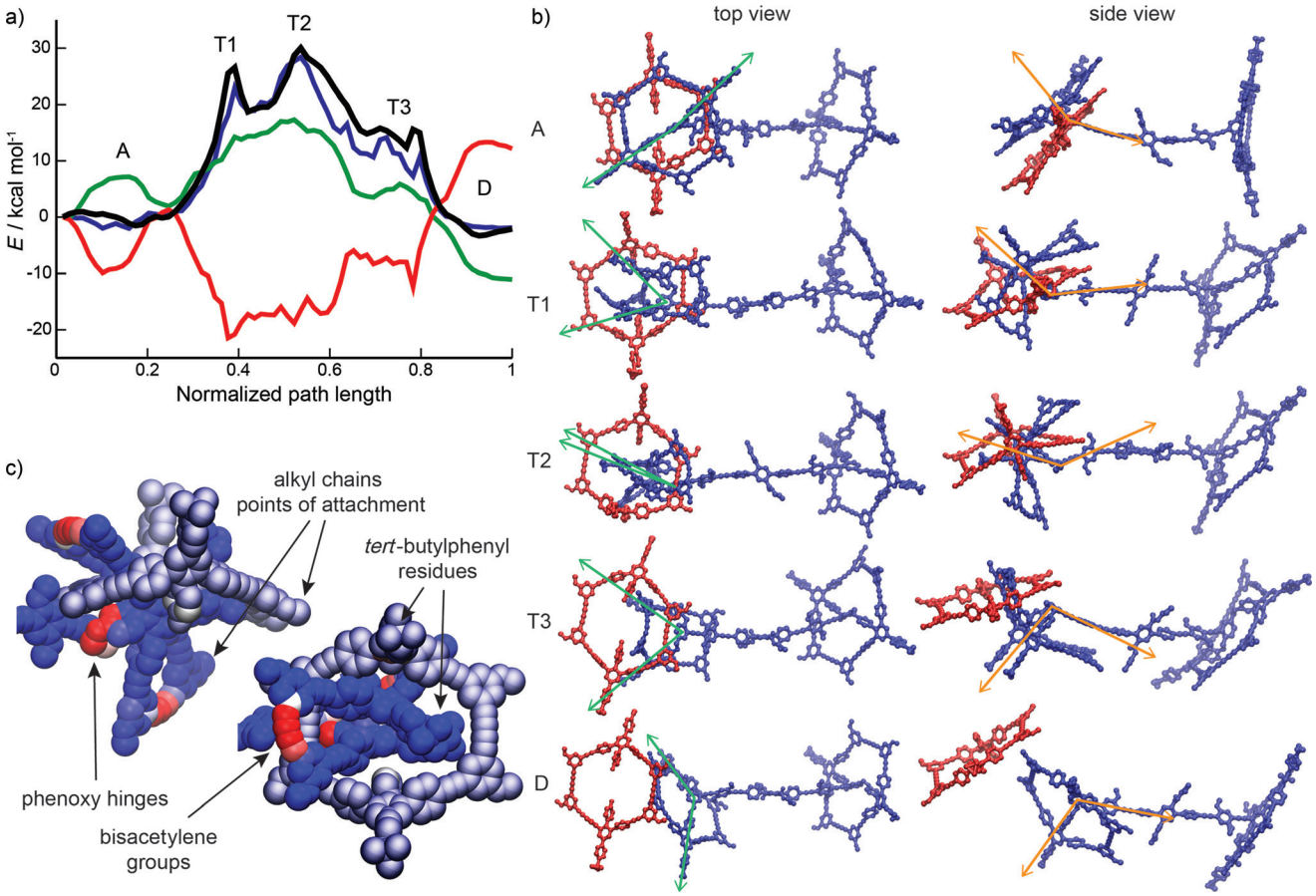

Figure 3. Theoretical description of the unthreading. a) Gibbs free energy (black line), entropy times temperature (red line), solvation free energy (green line), and bonding part of the enthalpy (blue line) of the optimized finite-temperature string. A: associated state, T1–T3: transition regions, D: dissociated state. b) Conformational changes during the unthreading. The axle is depicted in blue and the wheel in red. The left and right columns show a top and a side view of the rotaxane, and the rows correspond to the regions in (a) according to the same naming convention. In the left column, the green vectors describe the angle formed by the phenyl rings of the stopper *tert*-butylphenyl residues and the phenyl group at the attachment point. This angle gradually decreases, which correlates with the stopper folding. During folding, strain builds up mainly in the bisacetylene and phenoxy groups, as shown in (c). In the right column, the orange vectors describe the angle between the axis and the bisector of the angle formed by the green vectors. This angle steadily increases and portrays the rotation of the stopper about the attachment point to the axis during the passage through the wheel opening. c) Van der Waals representation of the transition state T2, in which only the actively participating wheel (metallic color) and stopper (full color) are depicted. The entire opening of the wheel is occupied by the bulky substituents of the stopper. The atom color depicts the change in the energy per atom with respect to the associated state (see the Supporting Information for a precise definition). The color ranges from blue to red as the magnitude of energy deviations increases. The red regions therefore correspond to hot spots of energy accumulation.

the phenoxy hinges connecting the stopper to the axis, and places a substantial strain on the unsaturated bisacetylene groups that build the sides of the stopper ring (Figure 3C). These conformational changes prepare the stage for the largest-scale motion: as the wheel steadily slips off the axis, and concomitantly with the stopper folding, the entire stopper macrocycle rotates about its attachment point to the axis (depicted by the orange vectors in Figure 3B) and passes through the wheel. Along this trajectory, the system goes through a couple of smaller barriers **T1** and **T3**, which mark the initial entry and final escape of the stopper from the wheel interior, and the transition state **T2**, in which the stopper occupies the entire opening of the wheel. The unthreading reaction thus involves large-scale collective conformational changes, which encompass virtually all atoms of the stopper and wheel macrocycles.

The deslipping process is predicted to be close to thermoneutral (Figure 3A). The highest of the transition states, **T2**, is roughly (30 ± 3.5) kcal mol^{-1} above the initial associated state and corresponds to the most spatially crowded conformation of the system. The computed free energy of activation is in a good agreement with the experimentally measured value of (24 ± 4) kcal mol^{-1}. The free energy was decomposed further into a sum of four contributions: the bonding and nonbonding enthalpy of the rotaxane, the solvation free energy, and the entropy multiplied by temperature. The bonding enthalpy is local because it accounts for the interactions between rotaxane atoms that are separated by no more than two neighbors, whereas the nonbonding enthalpy contains the interactions of distant atomic pairs. The sum of these two terms equals the total rotaxane enthalpy change, and three out of the four contri-

butions (all but the nonbonding enthalpy) are shown in Figure 3A.

As the system approaches the transition state **T2** from the side of the associated state, the entropy decreases because of the reduced conformational freedom of the crowded bottleneck region. Past the transition, the entropy increases and partly compensates the energetic losses incurred in the breaking of noncovalent interactions. The solvent free energy follows a similar trend: initially, the rotaxane desolvates because of the crowding, and then it solvates again as the stopper leaves the wheel. Remarkably, the entropy and solvation free energy nearly compensate the nonbonding enthalpy (not shown in Figure 3A), and thus the remaining part, the bonding enthalpy, determines the free-energy profile of the unthreading (Figure 3A). This energy compensation has important consequences for the influence of structural changes on the unthreading. Local modifications, which affect mainly the bonding enthalpy, are the main candidates for fine control of the disassembly. On the other hand, structural variations related to steric crowding of the transition states exhibit the "all-or-nothing" effect.[19] Such variations either completely abort disassembly or barely influence it. Finally, solvation alone provides a way of varying the activation barrier: if the absolute solvation energy of the rotaxane increases, the desolvation of the transition state becomes more costly.

In summary, we synthesized two novel phenylacetylene-based [2]rotaxanes, in which both the wheel and the bulky stoppers are phenylene–ethynylene–butadiynylene macrocycles of the same size. The stoppers are large enough to enable the synthesis, purification, and characterization of the rotaxanes. However, the wheel unthreads from the axis at 60 °C with a half-life of about 10 h. We described theoretically the unthreading by state-of-the-art DFT-based molecular-mechanics models and a string-based method for the simulation of rare events. This approach enabled us to characterize in detail the mechanism of the deslipping process and to determine the residues controlling the disassembly timescale. We demonstrated for the first time the use of molecular simulation to gain insight into the intricate dynamics of molecular nanoarchitectures that defy intuitive geometrical considerations.

Acknowledgements

Financial support by the Fonds der Chemischen Industrie (FCI) is gratefully acknowledged. P.S. acknowledges support from the Alexander von Humboldt Foundation.

Keywords: density functional calculations · interlocked systems · molecular modeling · rotaxanes · template synthesis

How to cite: *Angew. Chem. Int. Ed.* **2016**, *55*, 3328–3333
Angew. Chem. **2016**, *128*, 3389–3394

[1] a) V. Balzani, A. Credi, F. M. Raymo, J. F. Stoddart, *Angew. Chem. Int. Ed.* **2000**, *39*, 3348–3391; *Angew. Chem.* **2000**, *112*, 3484–3530; b) C. A. Schalley, K. Beizai, F. Vögtle, *Acc. Chem. Res.* **2001**, *34*, 465–476; c) N. C. Seeman, *Annu. Rev. Biochem.* **2010**, *79*, 65–87; d) S. F. M. van Dongen, S. Cantekin, J. A. A. W. Elemans, A. E. Rowan, R. J. M. Nolte, *Chem. Soc. Rev.* **2013**, *42*, 99; e) E. A. Neal, S. M. Goldup, *Chem. Commun.* **2014**, *50*, 5128–5142; f) K. Kinbara, T. Aida, *Chem. Rev.* **2005**, *105*, 1377–1400.

[2] a) I. T. Harrison, S. Harrison, *J. Am. Chem. Soc.* **1967**, *89*, 5723–5724; b) G. Schill, H. Zollenkopf, *Justus Liebigs Ann. Chem.* **1969**, *721*, 53–74; c) D. B. Amabilino, J. F. Stoddart, *Chem. Rev.* **1995**, *95*, 2725–2828; d) J.-P. Sauvage, C. O. Dietrich-Buchecker, *Molecular Catenanes, Rotaxanes, and Knots: A Journey Through the World of Molecular Topology*, Wiley-VCH, Weinheim, **1999**; e) M. Xue, Y. Yang, X. Chi, X. Yan, F. Huang, *Chem. Rev.* **2015**, *115*, 7398–7501.

[3] a) E. R. Kay, D. A. Leigh, F. Zerbetto, *Angew. Chem. Int. Ed.* **2007**, *46*, 72–191; *Angew. Chem.* **2007**, *119*, 72–196; b) J. D. Badjic, V. Balzani, A. Credi, S. Silvi, J. F. Stoddart, *Science* **2004**, *303*, 1845–1848; c) M. J. Frampton, H. L. Anderson, *Angew. Chem. Int. Ed.* **2007**, *46*, 1028–1064; *Angew. Chem.* **2007**, *119*, 1046–1083; d) B. Lewandowski, G. De Bo, J. W. Ward, M. Papmeyer, S. Kuschel, M. J. Aldegunde, P. M. E. Gramlich, D. Heckmann, S. M. Goldup, D. M. D'Souza, A. E. Fernandes, D. A. Leigh, *Science* **2013**, *339*, 189–193; e) S. Erbas-Cakmak, D. A. Leigh, C. T. McTernan, A. L. Nussbaumer, *Chem. Rev.* **2015**, *115*, 10081–10206.

[4] a) R. Hoss, F. Vögtle, *Angew. Chem. Int. Ed. Engl.* **1994**, *33*, 375–384; *Angew. Chem.* **1994**, *106*, 389–398; b) F. Diederich, P. J. Stang, *Templated Organic Synthesis*, Wiley-VCH, Weinheim, **2000**; c) T. J. Hubin, D. H. Busch, *Coord. Chem. Rev.* **2000**, *200–202*, 5–52; d) F. Arico, J. D. Badjic, S. J. Cantrill, A. H. Flood, K. C.-F. Leung, Y. Liu, J. F. Stoddart, *Top. Curr. Chem.* **2005**, *249*, 203–259.

[5] a) C. A. Hunter, *J. Am. Chem. Soc.* **1992**, *114*, 5303–5311; b) F. Vögtle, S. Meier, R. Hoss, *Angew. Chem. Int. Ed. Engl.* **1992**, *31*, 1619–1622; *Angew. Chem.* **1992**, *104*, 1628–1631.

[6] a) C. O. Dietrich-Buchecker, J.-P. Sauvage, J. P. Kintzinger, *Tetrahedron Lett.* **1983**, *24*, 5095–5098.

[7] a) P. R. Ashton, T. T. Goodnow, A. E. Kaifer, M. V. Reddington, A. M. Z. Slawin, N. Spencer, J. F. Stoddart, C. Vicent, D. J. Williams, *Angew. Chem. Int. Ed. Engl.* **1989**, *28*, 1396–1399; *Angew. Chem.* **1989**, *101*, 1404–1408.

[8] a) G. Wenz, B.-H. Han, A. Müller, *Chem. Rev.* **2006**, *106*, 782–817; b) A. Harada, Y. Takashima, H. Yamaguchi, *Chem. Soc. Rev.* **2009**, *38*, 875.

[9] a) G. Schill, A. Lüttringhaus, *Angew. Chem. Int. Ed. Engl.* **1964**, *3*, 546–547; *Angew. Chem.* **1964**, *76*, 567–568.

[10] a) Ö. Ünsal, A. Godt, *Chem. Eur. J.* **1999**, *5*, 1728–1733; b) A. Godt, *Eur. J. Org. Chem.* **2004**, 1639–1654.

[11] a) K. Hiratani, J. Suga, Y. Nagawa, H. Houjou, H. Tokuhisa, M. Numata, K. Watanabe, *Tetrahedron Lett.* **2002**, *43*, 5747–5750; b) K. Hiratani, M. Kaneyama, Y. Nagawa, E. Koyama, M. Kanesato, *J. Am. Chem. Soc.* **2004**, *126*, 13568–13569; c) N. Kameta, K. Hiratani, Y. Nagawa, *Chem. Commun.* **2004**, 466–467.

[12] K. Hirose, K. Nishihara, N. Harada, Y. Nakamura, D. Masuda, M. Araki, Y. Tobe, *Org. Lett.* **2007**, *9*, 2969–2972.

[13] a) H. Kawai, T. Umehara, K. Fujiwara, T. Tsuj, T. Suzuki, *Angew. Chem. Int. Ed.* **2006**, *45*, 4281–4286; *Angew. Chem.* **2006**, *118*, 4387–4392.

[14] K. Cantin, A. Lafleur-Lambert, P. Dufour, J.-F. Morin, *Eur. J. Org. Chem.* **2012**, 5335–5349.

[15] a) M. R. Panman, P. Bodis, D. J. Shaw, B. H. Bakker, A. C. Newton, E. R. Kay, A. M. Brouwer, W. J. Buma, D. A. Leigh, S. Woutersen, *Science* **2010**, *328*, 1255–1258; b) Q. Gan, Y. Ferrand, C. Bao, B. Kauffmann, A. Grelard, H. Jiang, I. Huc,

Science **2011**, *331*, 1172 – 1175; c) W. R. Browne, B. L. Feringa, *Nat. Nanotechnol.* **2006**, *1*, 25 – 35.

[16] a) S. Höger, *J. Polym. Sci. Part A* **1999**, *37*, 2685 – 2698; b) M. M. Haley, J. J. Pak, S. C. Brand, *Top. Curr. Chem.* **1999**, *201*, 81 – 129; c) U. H. F. Bunz, Y. Rubin, Y. Tobe, *Chem. Soc. Rev.* **1999**, *28*, 107 – 119; d) C. Grave, A. D. Schlüter, *Eur. J. Org. Chem.* **2002**, 3075 – 3098; e) W. Zhang, J. S. Moore, *Angew. Chem. Int. Ed.* **2006**, *45*, 4416 – 4439; *Angew. Chem.* **2006**, *118*, 4524 – 4548; f) S. Höger, *Pure Appl. Chem.* **2010**, *82*, 821 – 830; g) M. Iyoda, J. Yamakawa, M. J. Rahman, *Angew. Chem. Int. Ed.* **2011**, *50*, 10522 – 10553; *Angew. Chem.* **2011**, *123*, 10708 – 10740.

[17] a) K. Becker, P. G. Lagoudakis, G. Gaefke, S. Höger, J. M. Lupton, *Angew. Chem. Int. Ed.* **2007**, *46*, 3450 – 3455; *Angew. Chem.* **2007**, *119*, 3520 – 3525; b) K. Becker, G. Gaefke, J. Rolffs, S. Höger, J. M. Lupton, *Chem. Commun.* **2010**, *46*, 4686 – 4688.

[18] S. Höger, A.-D. Meckenstock, *Chem. Eur. J.* **1999**, *5*, 1686 – 1691.

[19] a) F. M. Raymo, K. N. Houk, J. F. Stoddart, *J. Am. Chem. Soc.* **1998**, *120*, 9318 – 9322; b) C. Heim, A. Affeld, M. Nieger, F. Vögtle, *Helv. Chim. Acta* **1999**, *82*, 746 – 759; c) G. M. Hübner, G. Nachtsheim, Q. Y. Li, C. Seel, F. Vögtle, *Angew. Chem. Int. Ed.* **2000**, *39*, 1269 – 1272; *Angew. Chem.* **2000**, *112*, 1315 – 1318.

[20] a) A. Affeld, G. M. Hübner, C. Seel, C. A. Schalley, *Eur. J. Org. Chem.* **2001**, 2877 – 2890; b) T. Felder, C. A. Schalley, *Angew. Chem. Int. Ed.* **2003**, *42*, 2258 – 2260; *Angew. Chem.* **2003**, *115*, 2360 – 2363; c) P. Linnartz, S. Bitter, C. A. Schalley, *Eur. J. Org. Chem.* **2003**, 4819 – 4829; d) S. Nygaard, B. W. Laursen, A. H. Flood, C. N. Hansen, J. O. Jeppesen, J. F. Stoddart, *Chem. Commun.* **2006**, 144 – 146; e) A. I. Prikhod'ko, J.-P. Sauvage, *J. Am. Chem. Soc.* **2009**, *131*, 6794 – 6807; f) Y. Akae, H. Okamura, Y. Koyama, T. Arai, T. Takata, *Org. Lett.* **2012**, *14*, 2226 – 2229.

[21] a) A. Onufriev, D. Bashford, D. A. Case, *Proteins Struct. Funct. Bioinf.* **2004**, *55*, 383 – 394; b) M. S. Lee, M. Feig, F. R. Salsbury, Jr., C. L. Brooks III, *J. Comput. Chem.* **2003**, *24*, 1348 – 1356; c) G. D. Hawkins, C. J. Cramer, D. G. Truhlar, *Chem. Phys. Lett.* **1995**, *246*, 122 – 129.

[22] a) S. Grimme, *J. Chem. Theory Comput.* **2014**, *10*, 4497 – 4514; b) TURBOMOLE V6.5 **2013**, a development of University of Karlsruhe and Forschungszentrum Karlsruhe GmbH, 1989 – 2007, TURBOMOLE GmbH, since **2007**; available from http://www.turbomole.com; c) J. Tao, J. P. Perdew, V. N. Staroverov, G. E. Scuseria, *Phys. Rev. Lett.* **2003**, *91*, 146401 – 146405; d) S. Grimme, J. Antony, S. Ehrlich, H. Krieg, *J. Chem. Phys.* **2010**, *132*, 154104; e) F. Weigend, R. Ahlrichs, *Phys. Chem. Chem. Phys.* **2005**, *7*, 3297 – 3305; f) A. Klamt, G. Schüürmann, *J. Chem. Soc. Perkin Trans. 2* **1993**, 799 – 805; g) F. Eckert, A. Klamt, COSMOtherm, Version C3.0, Release 15.01; COSMOlogic GmbH & Co. KG, Leverkusen, Germany, **2014**; F. Eckert, A. Klamt, *AIChE J.* **2002**, *48*, 369; h) the molecular Hessian was computed at the TPSS-D3/def2-SV(P) level of theory, and the single-point DFT energies were calculated at TPSS-D3/def2-TZVP(-f) level together with COSMO-RS for the solvation free energy; i) W. Humphrey, A. Dalke, K. Schulten, *J. Mol. Graphics* **1996**, *14*, 33 – 38.

[23] a) W. E, W. Ren, E. Vanden-Eijnden, *Chem. Phys. Lett.* **2005**, *413*, 242 – 247; b) W. E, W. Ren, E. Vanden-Eijnden, *Phys. Rev. B* **2002**, *66*, 052301; c) W. Ren, E. Vanden-Eijnden, P. Maragakis, *J. Chem. Phys.* **2005**, *123*, 134109 – 12; d) V. Ovchinnikov, M. Karplus, *J. Chem. Phys.* **2014**, *140*, 175103 – 18.

[24] http://www.thch.uni-bonn.de/tc/index.php?section = downloads&subsection = movies_rotaxane&lang = english.

Received: October 23, 2015
Revised: December 8, 2015
Published online: February 2, 2016

